Resonant Auger–intersite-Coulombic hybridized decay in the photoionization of endohedral fullerenes

Mohammad H. Javani,[1] Jacob B. Wise,[2] Ruma De,[2] Mohamed E. Madjet,[3] Steven T. Manson,[1] and Himadri S. Chakraborty[2,*]

[1]*Department of Physics and Astronomy, Georgia State University, Atlanta, Georgia 30303, USA*
[2]*Department of Natural Sciences, Center for Innovation and Entrepreneurship,*
Northwest Missouri State University, Maryville, Missouri 64468, USA
[3]*Qatar Energy and Environment Research Institute (QEERI), P.O. Box 5825, Doha, Qatar*

Considering the photoionization of $Ar@C_{60}$, we predict resonant femtosecond decays of both Ar and C_{60} vacancies through the continua of atom-fullerene hybrid final states. For Ar $3s \rightarrow np$ excitations, these resonances are far stronger than the Ar-to-C_{60} resonant intersite-Coulombic decays (ICD), while for C_{60} excitations they are strikingly larger than the corresponding Auger features. The results indicate the power of hybridization to enhance decay rates and modify lifetimes and line profiles, offering a unique probe, more powerful than regular ICDs, for multicenter decay processes.

PACS number(s): 33.80.Eh, 36.40.Cg, 61.48.−c

Intersite-Coulombic decay (ICD), originally predicted by Cederbaum *et al.* [1] and observed initially for Ne clusters [2], is a nonradiative relaxation pathway of a vacancy in atom A in a cluster or molecule. An outer electron of A fills the vacancy and the released energy, instead of emitting a second electron of A as in ordinary Auger ionization, transfers to a neighboring atom B *via* Coulomb interactions to ionize B. Repulsion between holes in A and B may lead to fragmentation. Over the last decade and a half, a wealth of theoretical [3] and experimental [4] research has gone into studying ICD in weakly bound atomic systems, such as rare gas dimers [5], rare gas clusters [6], surfaces [7], and water droplets [8,9]. ICD following the resonant Auger decay is identified in Ar dimers using momentum resolved electron-ion-ion coincidence spectroscopy [10,11]. Ultrafast ICDs of a dicationic monomer in a cluster to produce a cluster trication [12] or multiply excited homoatomic cluster [13] were predicted. Time-domain measurements of ICD in He [14] and Ne [15] dimers have recently been achieved. Besides interests in novel spectroscopy, low-energy ICD electrons find potential applications in radio-oncology [16,17].

Of particular interest is the resonant ICD (RICD) where the precursor excitation to form an inner-shell vacancy is accomplished by promoting an inner electron to an excited state by an external stimulant, generally electromagnetic radiation [18,19], or more recently, charge-particle impact [20]. A study of RICD followed by Ne $2s \rightarrow np$ excitations in MgNe clusters predicted its leading contribution among other interatomic decay modes [21]. RICD signatures were measured in photoelectron spectroscopy with Ne clusters for $2s \rightarrow np$ excitations [18] and in the double photoionization of Ne dimers by tracking the formation of energetic Ne^+ fragments [19]. Most recently, strong enhancement of the $HeNe^+$ yield, as He resonantly couples with the radiation, is detected [22], confirming an earlier prediction [23].

Atoms confined in fullerenes forming endofullerene compounds are attractive natural laboratories to study RICD processes. There are two compelling reasons for this: (i) such

materials are highly stable, have low-cost sustenance at the room temperature, and are enjoying a rapid improvement in synthesis techniques [24]; and (ii) the effect of correlation of the central atom with the cage electrons is predicted to spectacularly affect the atomic photoionization [25]. Moreover, endofullerene materials carry broad applied relevance [24].

A first attempt to predict ICD in endofullerenes was made by calculating ICD rates for $Ne@C_{60}$ [26]. While some speculations on the role of Coulomb-mediated energy transfer from atom to fullerene to broaden Auger lines were made [27,28], no studies—theoretical or experimental—of RICD resonances in the ionization of endofullerenes have been performed. On the other hand, ICD of these molecules can uncover effects not yet known. This is because (i) endofullerenes being spherical and asymmetric dimers of an atom and a cluster can readily induce reverse RICD processes, the decay of cluster innershell excitations through the continuum of the confined atom; and, far more importantly, (ii) possibilities of atom-fullerene hybridized final states, predicted to exist abundantly in these systems [29,30], can vastly alter the landscape of multicenter decay processes.

In this article, we show that for an Ar atom sequestered in C_{60}, ICD pathways of photogenerated inner-shell holes, both in Ar and C_{60}, can coherently mix with degenerate *intrasite* Auger pathways to produce final states with *shared* holes in atom-fullerene hybrid levels. Figure 1, a schematic of the process, illustrates this hitherto undetected mode that can be called the resonant hybrid Auger–intersite-Coulombic decay or RHA-ICD.

A jellium-based time-dependent local density approximation (TDLDA), with the van Leeuwen and Baerends (vLB) exchange-correlation functional to produce accurate asymptotic behavior [31] for ground and continuum states, is employed to calculate the dynamical response of the system to the incident photon. The Ar nucleus is placed at the center of the sphere where the chemically inert noble gas atom is known to localize. In solving the Kohn-Sham equations to obtain the ground state, a few optimizations were adopted [32]. The model enjoyed earlier successes in detecting a volume-type plasmon in C_{60} [33], interpreting the energy-dependent oscillations in C_{60} valence photointensity

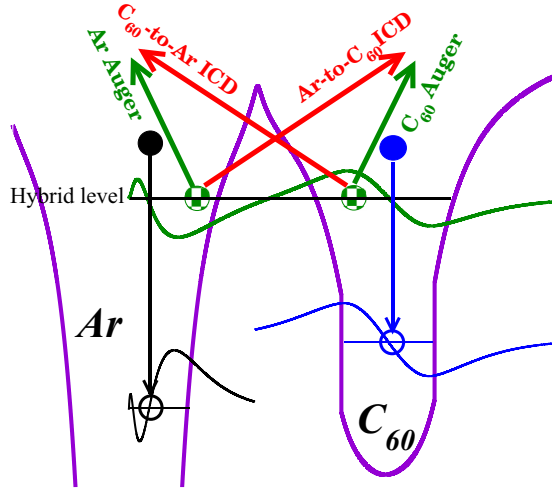_____
*himadri@nwmissouri.edu

FIG. 1. (Color online) Schematic of coherent mixing of one-center Auger decays (green) of core holes with corresponding ICDs (red) in the spectra of Ar-C_{60} hybrid electrons.

data [34], and predicting giant enhancements in the confined atom's response from its coupling with C_{60} plasmons [25]. Significant ground-state hybridization of Ar $3p$ orbital with C_{60} $3p$ is found, resulting in $(Ar+C_{60})3p$ and $(Ar-C_{60})3p$ levels from the symmetric and antisymmetric mixing (analogs of bonding and antibonding states in molecules or dimers):

$$(Ar\pm C_{60})3p = |\phi_{\pm}\rangle = \sqrt{\alpha}|\phi_{3pAr}\rangle \pm \sqrt{1-\alpha}|\phi_{3pC_{60}}\rangle, \quad (1)$$

where $\alpha \simeq 0.5$. Such atom-fullerene hybridization was predicted earlier [29] and detected in a photoemission experiment on multilayers of Ar@C_{60} [35]. In fact, the hybridization gap of 1.52 eV between $(Ar+C_{60})3p$ and $(Ar-C_{60})3p$ in our calculation is in good agreement with the measured value of 1.6±0.2 eV [35]. Our TDLDA+vLB scheme has recent success in the time-domain ionization of these hybrid electrons [36]. We use the symbol $n\ell@$ to denote the levels of the confined atom and $@n\ell$ to represent the levels of the doped C_{60}.

Figure 2 shows the $3p$ photoionization cross section of free Ar using TDLDA. Two Auger window resonances at 27.2 and 28.6 eV correspond to regular autoionizing states formed by two lowest inner-shell excitations $3s \rightarrow 4p, 5p$. We also present in Fig. 2 the cross sections for C_{60} @$7h$, the highest occupied (HOMO) level of C_{60} π symmetry (one radial node), and for @$2s$, the bottom level of the π band. Both these cross sections exhibit a host of routine autoionizing resonances corresponding to C_{60} inner-shell excitations which also appear in the C_{60} total cross section (shown). Three rather weak features, labeled as A, B, and C, are noted in the @$7h$ and @$2s$ curves which do not have partners in the free C_{60} cross section, however. These are Ar-to-C_{60} ICD resonances, resulting from the decay of Ar $3s@$ vacancies from $3s@ \rightarrow 3p@, 4p@, 5p@$ excitations through C_{60} @$7h$ and @$2s$ continua. Slight redshifts of these resonances from their free Ar counterparts are due to some adjustments in $3s$ ground and np excited energies from confinement. Evidently, TDLDA predicts extremely weak ICD rates whose measurement is a clear challenge.
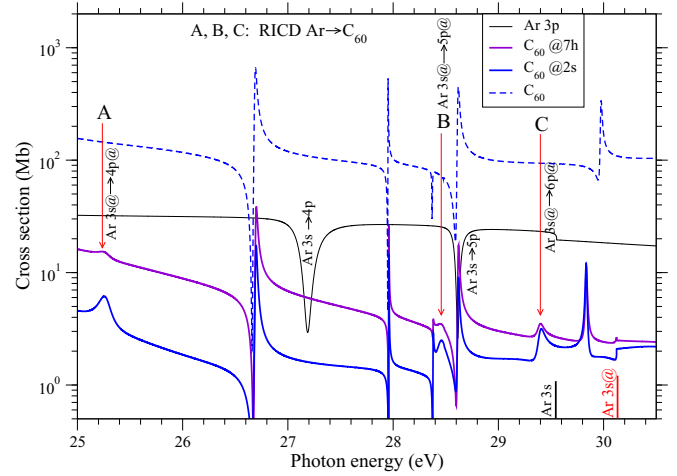

FIG. 2. (Color online) Photoionization cross sections of free Ar $3p$ and empty C_{60} compared with the results for C_{60} @$7h$ and @$2s$ levels in Ar@C_{60}. Three Ar-to-C_{60} ICD resonances (labeled as A,B,C) amongst regular autoionizing resonances are identified in the C_{60} @$7h$ and @$2s$ cross sections.

Figure 3 displays cross sections, over the same energy range of Fig. 2, for the endofullerene hybrid levels $(Ar\pm C_{60})3p$. Features A, B, and C in these curves are resonances that emerge from the decay of $3s@ \rightarrow 3p@, 4p@, 5p@$ excitations through the continuum of these hybrid levels. The features are similar in shape to the autoionizing resonances in free Ar $3p$ (included in Fig. 3) and appear at the same Ar-to-C_{60} RICD energies (Fig. 2). Remarkably, they are significantly stronger, particularly for $(Ar-C_{60})3p$, than the Ar-to-C_{60} RICDs. Another dramatic effect can be noted: The empty C_{60} $3p$ cross section in Fig. 3 shows autoionizing resonances corresponding to Auger decays of C_{60} inner-shell vacancies. But the structures at the corresponding energies in hybrid channels from the decay of C_{60} vacancies are order of magnitude larger than the autoionizing resonances in empty C_{60}. We particularly identify the resonances labeled as 1–4 in Fig. 3. In essence, Ar and C_{60} inner-shell vacancies decay significantly more powerfully through the photoionization
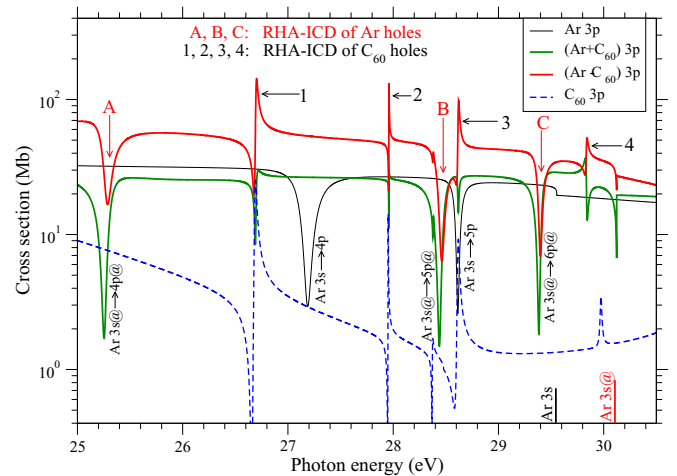

FIG. 3. (Color online) Photoionization cross sections of free Ar $3p$ and C_{60} $3p$ levels compared with those of their hybrid pair.

continua of Ar-C_{60} hybrid levels than through the continua of pure C_{60} levels. These resonances are qualitatively different from the standard RICD. We show that they emerge from a coherent interference between resonant Auger and ICD channels that produce *divided* vacancies in the final state, vacancies shared by the confined Ar and the confining C_{60}.

The TDLDA matrix elements for the dipole photoionization of $(Ar\pm C_{60})3p$, in the interchannel coupling frame introduced by Fano [37], can be written as [38]

$$\mathcal{M}_\pm(E) = \mathcal{D}_\pm(E) + M_\pm^{c\text{-}c}(E) + M_\pm^{d\text{-}c}(E), \qquad (2)$$

where the single electron (LDA) matrix element $\mathcal{D}_\pm(E) = \langle ks(d)|z|\phi_\pm\rangle$; $M^{c\text{-}c}$ and $M^{d\text{-}c}$ are, respectively, corrections from continuum-continuum and bound-continuum channel couplings. $M^{c\text{-}c}$ constitutes a rather smooth many-body contribution to nonresonant cross section [30], while the resonance structures originate from $M^{d\text{-}c}$. Following Ref. [37],

$$M_\pm^{d\text{-}c} = \sum_{n\ell} \sum_{\eta\lambda} \frac{\langle\psi_{n\ell\to\eta\lambda}|\frac{1}{|\mathbf{r}_\pm - \mathbf{r}_{n\ell}|}|\psi_\pm(E)\rangle}{E - E_{n\ell\to\eta\lambda}} \mathcal{D}_{n\ell\to\eta\lambda}, \quad (3)$$

in which $|\psi\rangle$ refer to interacting discrete $n\ell \to \eta\lambda$ and continuum $(Ar\pm C_{60})3p \to ks(d)$ *channel* wave functions; $E_{n\ell\to\eta\lambda}$ and $\mathcal{D}_{n\ell\to\eta\lambda}$ are LDA bound-to-bound excitation energies and matrix elements, respectively. The excited states of the system are found hybridized, implying that inner-shell electrons from pure levels are excited to the hybrid levels. But we do not expect significant differences in $\mathcal{D}_{3s\to\eta p}$ between free and confined Ar. This is because, even though hybrid excited waves have structures in the C_{60} shell, the Ar $3s$ wave function localized on Ar (Fig. 1) practically does not affect the overlaps. An identical reason also ensures effectively unchanged C_{60} inner excitation matrix elements from the doping.

Following Eqs. (1), the hybridization of the continuum channels in Eq. (3) assumes the form

$$|\psi_\pm\rangle = \sqrt{\alpha}|\psi_{3p@Ar}\rangle \pm \sqrt{1-\alpha}|\psi_{@3pC_{60}}\rangle. \qquad (4)$$

In Eq. (4) we used @ to indicate modifications of the continuum waves in confined Ar and doped C_{60}. Using Eq. (4) in (3), and recognizing that the overlap between a pure Ar and a pure C_{60} bound state is negligible, we separate the atomic and fullerene regions of integration:

$$M_\pm^{d\text{-}c}(E) = \sum_{n\ell} \sum_{\eta\lambda} \left[\sqrt{\alpha} \frac{\langle\psi_{n\ell\to\eta\lambda}|\frac{1}{|\mathbf{r}_\pm - \mathbf{r}_{n\ell}|}|\psi_{3p@Ar}(E)\rangle}{E - E_{n\ell\to\eta\lambda}} \right.$$
$$\left. \pm \sqrt{1-\alpha} \frac{\langle\psi_{n\ell\to\eta\lambda}|\frac{1}{|\mathbf{r}_\pm - \mathbf{r}_{n\ell}|}|\psi_{@3pC_{60}}(E)\rangle}{E - E_{n\ell\to\eta\lambda}} \right] \mathcal{D}_{n\ell\to\eta\lambda}. \qquad (5)$$

Obviously, if $n\ell \to \eta\lambda$ produces Ar inner-shell holes, resulting to resonances A, B, and C in Fig. 3, then the first term on the right-hand side of Eq. (5) represents the ordinary intrasite Auger decay in Ar, while the second term denotes the Ar-to-C_{60} RICD. Conversely, for C_{60} inner vacancies (resonances 1–4 in Fig. 3), the first and second terms, respectively, present reverse RICD (C_{60}-to-Ar) and C_{60} Auger processes. These decays are schematically shown in Fig. 1.

For the cross sections, which involve the modulus squared of the matrix element, two key mechanisms play out: First,

Auger and ICD pathways in Eq. (5) combine coherently to induce resonances, allowing shared outer-shell vacancies. Hence, this decay pathway can be called RHA-ICD. Note that both the terms in Eq. (5) are large, owing to substantial overlaps between innershell bound states and $(Ar\pm C_{60})3p$ wave functions. This partly explains why the features identified in Fig. 3 are stronger than corresponding autoionizing and ICD resonances. Second, the resonances in the matrix element $M_\pm^{d\text{-}c}$ also interfere with the nonresonant part $\mathcal{D}_\pm + M_\pm^{c\text{-}c}$ [Eq. (2)], which is generally stronger for hybrid levels than pure C_{60} levels [30]. This interference further enhances RHA-ICD resonances compared to their Auger partners in empty C_{60}, as seen for structures 1–4 in Fig. 3. The results exhibit completely different resonance shapes for Ar-to-C_{60} RICDs (Fig. 2) compared to corresponding RHA-ICDs (Fig. 3), although their lifetimes increase only slightly. Noticeably, the lifetime (130 fs) of the Auger feature 1 decreases to about 40 fs for the respective RHA-ICDs (Fig. 3), while there is a strong shape alteration for the feature 4.

The present results are based on participant RICD processes only, as the spectator RICD is not included within TDLDA. However, the spectator channels are likely to see an even stronger RHA-ICD decay primarily due to their known higher RICD strength [16], i.e., the inclusion of spectator RICD is likely to further enhance the effects discussed. Also, hybrid final-state vacancies may have unique consequences for the spectator type RHA-ICD: the postdecay repulsive force will considerably increase compared to RICD, since a half vacancy will reside too close to a full vacancy either on Ar or on C_{60}, allowing stronger fragmentation forces.

Enhancement of ICD rates from orbital mixing was earlier found in aqueous hydroxides [39], which are far more complex systems than endofullerenes. However, similar results in two such vastly different systems imply a general trend of the effect, providing its wider context in experimental and theoretical research.

RICD systems are visualized as natural antenna-receiver pairs at the molecular scale [22] where the antenna couples to the incoming photon and transfers energy to the receiver to perform. RHA-ICD processes, predicted here, can enhance the efficiency of the ultimate output by enabling the antenna to also contribute to the emission resonantly with the receiver through a quantum coherence. The effect may have significant utilization in nanoscale antenna technology [40].

In conclusion, we used the TDLDA methodology to calculate a variety of resonances in the photoionization of Ar@C_{60} that includes Ar-to-C_{60} ICD resonances. A different class of resonances decaying into atom-fullerene hybrid final-state vacancies is found which arises from the competition of the intersite-Coulombic autoionizing channel with an intrinsically connected intrasite Auger channel. These resonances are remarkably stronger than both regular ICD and Auger resonances, hence experimentally detectable, allowing a singularly powerful access path to ICD activities. They are likely to also exist generally in the continuum of molecules, nanodimers and nanopolymers, and fullerene onions that support hybridized electrons as well.

[1] L. S. Cederbaum, J. Zobeley, and F. Tarantelli, Phys. Rev. Lett. **79**, 4778 (1997).

[2] S. Marburger, O. Kugeler, U. Hergenhahn, and T. Möller, Phys. Rev. Lett. **90**, 203401 (2003).

[3] V. Averbukh, Ph. V. Demekhinb, P. Kolorenc, S. Scheitd, S. D. Stoycheve, A. I. Kuleff, Y.-C. Chiange, K. Gokhberge, S. Kopelkee, N. Sisourate, and L. S. Cederbaume, J. Electron Spectrosc. Relat. Phenom. **183**, 36 (2011).

[4] U. Hergenhahn, J. Electron Spectrosc. Relat. Phenom. **184**, 78 (2011).

[5] T. Jahnke, A. Czasch, M. S. Schöffler, S. Schössler, A. Knapp, M. Käsz, J. Titze, C. Wimmer, K. Kreidi, R. E. Grisenti, A. Staudte, O. Jagutzki, U. Hergenhahn, H. Schmidt-Böcking, and R. Dörner, Phys. Rev. Lett. **93**, 163401 (2004).

[6] G. Öhrwall, M. Tchaplyguine, M. Lundwall, R. Feifel, H. Bergersen, T. Rander, A. Lindblad, J. Schulz, S. Peredkov, S. Barth, S. Marburger, U. Hergenhahn, S. Svensson, and O. Björneholm, Phys. Rev. Lett. **93**, 173401 (2004).

[7] G. A. Grieves and T. M. Orlando, Phys. Rev. Lett. **107**, 016104 (2011).

[8] T. Jahnke, H. Sann, T. Havermeier, K. Kreidi, C. Stuck, M. Meckel, M. Schöffler, N. Neumann, R. Wallauer, S. Voss, A. Czasch, O. Jagutzki, A. Malakzadeh, F. Afaneh, Th. Weber, H. Schmidt-Böcking, and R. Dörner, Nat. Phys. **6**, 139 (2010).

[9] M. Mucke, M. Braune, S. Barth, M. Förstel, T. Lischke, V. Ulrich, T. Arion, U. Becker, A. Bradshaw, and U. Hergenhahn, Nat. Phys. **6**, 143 (2010).

[10] P. O'Keeffe, E. Ripani, P. Bolognesi, M. Coreno, M. Devetta, C. Callegari, M. Di Fraia, K. C. Prince, R. Richter, M. Alagia, A. Kivimäki, and L. Avaldi, Phys. Chem. Lett. **4**, 1797 (2013).

[11] M. Kimura, H. Fukuzawa, K. Sakai, S. Mondal, E. Kukk, Y. Kono, S. Nagaoka, Y. Tamenori, N. Saito, and K. Ueda, Phys. Rev. A **87**, 043414 (2013).

[12] R. Santra and L. S. Cederbaum, Phys. Rev. Lett. **90**, 153401 (2003).

[13] A. I. Kuleff, K. Gokhberg, S. Kopelke, and L. S. Cederbaum, Phys. Rev. Lett. **105**, 043004 (2010).

[14] F. Trinter, J. B. Williams, M. Weller, M. Waitz, M. Pitzer, J. Voigtsberger, C. Schober, G. Kastirke, C. Müller, C. Goihl, P. Burzynski, F. Wiegandt, T. Bauer, R. Wallauer, H. Sann, A. Kalinin, L. Ph.H. Schmidt, M. Schöffler, N. Sisourat, and T. Jahnke, Phys. Rev. Lett. **111**, 093401 (2013).

[15] K. Schnorr, A. Senftleben, M. Kurka, A. Rudenko, L. Foucar, G. Schmid, A. Broska, T. Pfeifer, K. Meyer, D. Anielski, R. Boll, D. Rolles, M. Kübel, M. F. Kling, Y. H. Jiang, S. Mondal, T. Tachibana, K. Ueda, T. Marchenko, M. Simon, G. Brenner, R. Treusch, S. Scheit, V. Averbukh, J. Ullrich, C. D. Schröter, and R. Moshammer, Phys. Rev. Lett. **111**, 093402 (2013).

[16] K. Gokhberg, P. Kolorenc, A. I. Kuleff, and L. S. Cederbaum, Nature (London) **505**, 661 (2014).

[17] F. Trinter, M. S. Schöffler, H.-K. Kim, F. P. Sturm, K. Cole, N. Neumann, A. Vredenborg, J. Williams, I. Bocharova, R. Guillemin, M. Simon, A. Belkacem, A. L. Landers, Th. Weber, H. Schmidt-Böcking, R. Dörner, and T. Jahnke, Nature (London) **505**, 664 (2014).

[18] S. Barth, S. Joshi, S. Marbuger, V. Ulrich, A. Lindblad, G. Öhrwall, O. Björneholm, and U. Hergenhahn, J. Chem. Phys. **122**, 241102 (2005).

[19] T. Aoto, K. Ito, Y. Hikosaka, E. Shigemasa, F. Penent, and P. Lablanquie, Phys. Rev. Lett. **97**, 243401 (2006).

[20] H.-K. Kim, H. Gassert, M. S. Schöffler, J. N. Titze, M. Waitz, J. Voigtsberger, F. Trinter, J. Becht, A. Kalinin, N. Neumann, C. Zhou, L. Ph. H. Schmidt, O. Jagutzki, A. Czasch, H. Merabet, H. Schmidt-Böcking, T. Jahnke, A. Cassimi, and R. Dörner, Phys. Rev. A **88**, 042707 (2013).

[21] K. Gokhberg, V. Averbukh, and L. S. Cederbaum, J. Chem. Phys. **124**, 144315 (2006).

[22] F. Trinter, J. B. Williams, M. Weller, M. Waitz, M. Pitzer, J. Voigtsberger, C. Schober, G. Kastirke, C. Müller, C. Goihl, P. Burzynski, F. Wiegandt, R. Wallauer, A. Kalinin, L. Ph. H. Schmidt, M. S. Schöffler, Y.-C. Chiang, K. Gokhberg, T. Jahnke, and R. Dörner, Phys. Rev. Lett. **111**, 233004 (2013).

[23] B. Najjari, A. B. Voitkiv, and C. Müller, Phys. Rev. Lett. **105**, 153002 (2010).

[24] A. A. Popov, S. Yang, and L. Dunsch, Chem. Rev. **113**, 5989 (2013).

[25] M. E. Madjet, H. S. Chakraborty, and S. T. Manson, Phys. Rev. Lett. **99**, 243003 (2007).

[26] V. Averbukh and L. S. Cederbaum, Phys. Rev. Lett. **96**, 053401 (2006).

[27] A. V. Korol and A. V. Solov'yov, J. Phys. B **44**, 085001 (2011).

[28] M. Ya. Amusia and A. S. Baltenkov, Phys. Rev. A **73**, 063206 (2006).

[29] H. S. Chakraborty, M. E. Madjet, T. Renger, Jan-M. Rost, and S. T. Manson, Phys. Rev. A **79**, 061201(R) (2009).

[30] J. N. Maser, M. H. Javani, R. De, M. E. Madjet, H. S. Chakraborty, and S. T. Manson, Phys. Rev. A **86**, 053201 (2012).

[31] R. van Leeuwen and E. J. Baerends, Phys. Rev. A **49**, 2421 (1994).

[32] M. E. Madjet, T. Renger, D. E. Hopper, M. A. McCune, H. S. Chakraborty, Jan-M. Rost, and S. T. Manson, Phys. Rev. A **81**, 013202 (2010).

[33] S. W. J. Scully, E. D. Emmons, M. F. Gharaibeh, R. A. Phaneuf, A. L. D. Kilcoyne, A. S. Schlachter, S. Schippers, A. Müller, H. S. Chakraborty, M. E. Madjet, and J. M. Rost, Phys. Rev. Lett. **94**, 065503 (2005).

[34] A. Rüdel, R. Hentges, U. Becker, H. S. Chakraborty, M. E. Madjet, and J. M. Rost, Phys. Rev. Lett. **89**, 125503 (2002).

[35] M. Morscher, A. P. Seitsonen, S. Ito, H. Takagi, N. Dragoe, and T. Greber, Phys. Rev. A **82**, 051201 (2010).

[36] G. Dixit, H. S. Chakraborty, and Mohamed El-Amine Madjet, Phys. Rev. Lett. **111**, 203003 (2013).

[37] U. Fano, Phys. Rev. **124**, 1866 (1961).

[38] M. H. Javani, M. R. McCreary, A. B. Patel, M. E. Madjet, H. S. Chakraborty, and S. T. Manson, Eur. Phys. J. D **66**, 189 (2012).

[39] C. P. Schwartz, S. Fatehi, R. J. Saykally, and D. Prendergast, Phys. Rev. Lett. **105**, 198102 (2010).

[40] L. Novotny and N. van Hulst, Nat. Photonics **5**, 83 (2012).